IgA dysfunctions induced by the early-lifetime disruption of gut microbitoa result in metabolic syndrome in mice

Jielong Guo
China Agricultural University
Xue Han
China Agricultural University
Yilin You
China Agricultural University
Weidong Huang
China Agricultural University
Zhan Jicheng (zhanjicheng@cau.edu.cn)
China Agricultural University https://orcid.org/0000-0001-8757-7862

Research

Keywords: IgA, gut microbiota, metabolic syndrome, Low-dose penicillin, fecal microbiota transplantation, probiotics

Posted Date: July 10th, 2020

DOI: https://doi.org/10.21203/rs.3.rs-40336/v1

Abstract

Backgroud: Disruption of the gut microbiota (GM), mainly induced by antibiotic treatments and C-sections, is prevalent during the early lifetime, which can result in lifelong changes in the GM composition and metabolism.

Results: The GM of newborn mice was influenced after being subjected to transitory treatment with low-dose penicillin (LDP), resulting in a permanent reduction of intestinal IgA. Germ-free (GF) mice transferred GM from the LDP-treated mice also showed decreased intestinal IgA levels. Similarly, antigens derived from the LDP-treated mice induced lower IgA production during in vitro incubation with small intestinal tissues. Furthermore, a lack of intestinal IgA led to the persistent dysbiosis of mucosal GM, causing metabolic syndrome (MetS) in the LDP-treated mice. The mice lacking intestinal IgA (*Pigr*$^{-/-}$) only showed transient alteration in GM after LDP exposure while the long-period metabolism was not influenced. Moreover, gavage with GM from the LDP-free mice or probiotics (partially) restored the GM and intestinal IgA, while improving the MetS in LDP-treated mice.

Conclusions: The antibiotics–induced changes of GM in early lifetime permanently dampened the IgA responses to the GM, which lead to the long-term dysbiosis of intestinal mucosal bacteria and MetS.

Introduction

The early-lifetime period is critical for the development of immunity and metabolism, since the correct colonization and maturation of GM are delicately controlled by the host, and has a lifelong impact on the health of the host [1–5]. The establishment and maturation of the infant GM can be disturbed by treatment with antibiotics (Abx), changes in diet (for example, nursing with formula), and the interruption of vaginal delivery (for example, birth by Caesarean section) [6]. The disruption of the neonatal microbiome can result in lifelong changes in the GM composition and has been linked to various conditions such as obesity, asthma, and inflammatory bowel disease (IBD) [7–10].

Since the GM composition changes significantly due to the alteration of diet and age, the question that requires clarification pertains to the force consistently driving different GM compositions in mice who experienced early-lifetime disruption. It has been reported that the period between 10 d to 21 d of age is a critical time during which the immune tolerance of mice to commensals is determined [5]. During this time window, the proper exposure to antigens allows for the establishment of immune tolerance [5]. Although the specific correlation between the antigen properties and the species of immunotolerant commensals has not been determined, some studies did show that a deficiency in the responses to certain bacteria resulted in the overrepresentation of these bacteria [11, 12]. Secreted by plasma cells, IgA plays a central role in actively controlling the GM composition in mice and humans [13–15]. An adult can produce several grams of IgA daily, most of which is secreted into the intestinal lumen in the form of secretory IgA (SIgA) [13]. Furthermore, ~ 60% of the bacteria in the small intestine are coated with IgA [16]. By binding to antigens in the intestine, IgA can prevent microbiota encroachment, reduce the

translocation of bacterial toxins, enhance the clearance of bacteria, and in some cases, facilitate their colonization [17, 18]. Moreover, the IgA response to certain microbes can continue for a long time (more than 3 months) following exposure, which can be attributed to the existence of memory IgA^+ B cells [11, 13].

Therefore, it could be speculated that IgA might play a pivotal role in mediating the prolonged influence of early-lifetime GM disturbance on metabolism. Here, we studied the role of IgA in the disruption of the GM and metabolism in a microbiota-induced metabolic syndrome (MetS) mouse mode as described before [3]. This model indicates that transient treatment of mice with low-dose Abx during early life results in the prolonged disruption of GM and MetS [3]. Meanwhile, the effects of the fecal microbiota transplantation (FMT) of probiotics on IgA production, GM, and metabolism were studied using this mouse model.

Results

Transient low-dose Abx treatment affected the early microbiota

From several days before birth to 30 d of age, some of the mice were treated with LDP (1.5 mg/kg body weight) (LDP), while the control (Ctr) group remained free of LDP administration to study its impact on intestinal microbiota. After the LDP treatment period, microbial DNA extracted from the luminal and mucosal ileum and colon samples were analyzed using V4 region sequencing.

Quantitative PCR (qPCR) using 16S universal or ITS1 primers[19] (Table S1) showed no significant differences between the bacterial counts or fungal loads of the LDP and Ctr intestinal samples, suggesting that the overall microbial loads were not influenced by LDP (Figures S1A–S1B). Nonetheless, significant differences were evident in the bacterial compositions of the ileal mucosa and colonic lumen of the LDP and Ctr mice, as shown by unweighted UniFrac distance measurements (Figures 1A and 1D). Similar trends were also found in the ileal lumen and colonic mucosa (Figures 1B and 1C). Linear discriminant analysis Effect Size (LEfSe) revealed several discrepant bacterial taxa enriched in each group (Figures 1E and S1C to S1E). Two dominant early life bacteria, namely *Lactobacillus* and *Candidatus Arthromitus* (segmented filamentous bacteria (SFB)), were enriched in all intestinal regions, including the mucosa and lumen of the ileum and colon in the Ctr group, but not in the LDP mice (Figures 1E and S1C to S1E). Moreover, bacterial taxa enriched in the LDP mice were more complicated and adult-like, including the taxa belonging to the phyla Bacteroidetes and Proteobacteria (Figures 1E and S1C to S1E). It is also worth noting that a more broad difference was observed between the ileal samples of the LDP and Ctr mice than that in colonic samples (Figures S1F and S1G).

Consistent with these observations, the abundance of SFB was significantly lower in the ileal mucosa and colonic lumen samples of LDP mice compared to that of Ctr mice (Figure 1F). Similar trends were also observed in the ileal lumen and colonic mucosa samples (Figure 1F). Furthermore, differences in the abundance of *Lactobacillus* in the LDP and Ctr mice were only evident in the ileal samples (Figure 1G). Since SFB and *Lactobacillus* are known to regulate intestinal immunity effectively [20, 21], we then

focused on the study of these two species. We firstly examined whether two approaches, namely FMT and probiotic intervention, which are commonly used for improving dysbiosis, could restore the abundance of SFB and *Lactobacillus*. Therefore, some of the LDP-treated pups were also treated several times with FMT (F group, fecal microbiota from the even-aged Ctr mice) or probiotics (P group), including *L. bulgaricus* and *L. rhamnosus* GG. Both probiotics could be identified in the mucosal samples and feces after the treatment through qPCR, suggesting that the probiotics had successfully colonized in the intestine (Figure S1H). Moreover, we found that FMT effectively restored the abundance of both SFB and *Lactobacillus,* while the probiotics only restored *Lactobacillus* (Figures 1F and 1G).

Changes in the microbiota led to a reduction in IgA production

SFB and *Lactobacillus* are known to induce the production of IgA [20, 21], the main host factor controlling intestinal microbiota. Therefore, a decrease in SFB and *Lactobacillus* in LDP mice may result in lower IgA levels in the small intestine, the primary location of IgA production [22]. In line to this, the caecal SIgA levels of the LDP mice were significantly lower than that of the Ctr mice at 30 d of age (Figure 2A). FMT treatment fully restored the caecal SIgA levels (Figure 2A), while probiotics could only accomplish partial restoration, which was consistent with the observation that probiotics failed to restore the SFB levels (Figure 1F). Furthermore, the immunofluorescence assay targeting the SIgA in the ileum produced consistent results (Figure 2C). The determination of the mRNA expression of genes related to SIgA production, including the TNF superfamily member 13b (*Tnfsf13b*, also known as BAFF), the immunoglobulin joining chain (*Jchain*), and the polymeric immunoglobulin receptor (*Pigr*) in the ileum showed that LDP inhibited the gene expression, which was (partially) restored by FMT and probiotics (Figures 2G and 2H). RNA-sequencing of the ileum also identified several biological functions related to IgA production that were downregulated in the LDP mice compared to the Ctr, F, and P groups, including PI3K signaling in B lymphocytes, B cell receptor signaling, and dendritic cell maturation (Figure 2J). Furthermore, no significant differences were evident in between the fecal SIgA levels of the LDP-treated and LDP-free mice at 14 d old or weaning age (Figure S2D), suggesting that the passive SIgA received from the breast milk of the dams were not influenced by LDP (mice begin to actively produce intestinal SIgA after weaning [7]). Interestingly, the caecal SIgA levels remained significantly lower in the 25-week old LDP mice compared to the sex-matched Ctr and F, but not the P mice (Figure 2B), suggesting the prolonged influence of early life LDP on IgA production.

Since both SFB and *Lactobacillus* belong to the phylum Firmicutes, we then aimed to determine the SIgA content responsible for targeting intestinal Firmicutes. To mimic the composition of intestinal Firmicutes as much as possible, we generated mice carrying GM composed of nearly “pure Firmicutes” using Abx or a high-fat diet (HFD) (60% energy from fat), or “no Firmicutes” using Abx (Figure S2A). As expected, employing antigens derived from the pooled (n = 3) cecal contents of these mice, we found that the LDP mice exhibited decreased levels of SIgA targeting antigens in both the HFD- and Abx-induced “pure Firmicutes” groups (Figure 2F). However, the LDP mice also showed decreased SIgA to antigens derived from the “no Firmicutes” group, which could possibly be attributed to the polyreactivity of IgA [23].

To further determine the correlation between LDP-induced intestinal microbiota disturbance and IgA reduction, we transferred fecal microbiota from 30-d-old Ctr, LDP, F, and P mice to even-aged germ free (GF) mice, and measured the fecal SIgA levels in recipients. Three days after transfer, the abundance of SFB and *Lactobacillus* in the LDP recipients (LDPR) were lower than in the Ctr recipients (CtrR), and the F recipients (FR) (Figures S2B and S2C). Three weeks post-transfer, LDPR exhibited significantly lower fecal SIgA levels compared to that of CtrR and FR, as well as the P recipients (PR) (Figure 2G). The difference in the fecal SIgA levels of the LDPR, CtrR, FR, and PR lasted six weeks after the transfer (Figure 2G). However, contrary to the donors, the fecal SIgA differences disappeared 12 weeks after the transfer (Figure 2G), suggesting that the time factor may play an important role in the prolonged effect of the IgA responses.

Finally, we examined the effect of the antigens derived from the Ctr, LDP, F, and P mice on IgA production during in vitro cultivation. Briefly, antigens derived from these mice were co-cultured with ileum tissue samples obtained from SPF C57/BL6 mice to study the effects of these antigens on ileal IgA production. The ileum tissue produced significantly more IgA when co-cultured with antigens derived from Ctr and F mice than from LDP mice (Figure 2H). A similar trend was evident for the antigens from the P mice compared to the LDP mice but did not reach significance (P = 0.094). Moreover, the mRNA expression of the *Jchain* of the ileum tissue was also higher when cultured with antigens derived from the Ctr and F mice than from the LDP mice (Figure 2I).

Collectively, these results showed that LDP-induced dysbiosis disturbed intestinal immunity and reduced intestinal IgA production, which could be (partially) restored by FMT and probiotics.

The IgA response dysfunction led to long-term dysbiosis

We then sought to determine the long-term influence of LDP on microbiota and its correlation with intestinal IgA. The bacterial composition of the ileal mucosa samples obtained from the 25-week-old LDP mice was significantly different from age- and sex-matched Ctr mice (Figures 3A and 3C). Similar trends were evident for the colonic mucosa samples but did not reach significant levels (p = 0.143 and 0.147 for males and females, respectively) (Figures 3B and 3D). Furthermore, no significant difference was apparent between the luminal bacterial compositions of the 25-week-old LDP and Ctr mice (Figures S3A–S3E). FMT treatment fully restored the LDP-induced disturbance caused by microbiota in the ileal mucosa (Figure 3F), while probiotics only partially achieved this goal, which was consistent with the influence of FMT and probiotics on intestinal SIgA (Figures 2B and 2C). Moreover, in line with the results that the LDP mice showed reduced intestinal IgA-targeted Firmicutes (Figure 2F), we also found a significant overrepresentation of this phylum in the mucosal samples of the 25-week-old LDP mice, which was fully reversed by FMT but only slightly by probiotics (only in the females) (Figure 3E). Furthermore, as with the modification of IgA production, the alteration of microbiota was also evident in LDPR mice six weeks after conventionalization (Figures 1G and S3G).

To further determine the correlations between IgA and microbiota, mice lacking intestinal IgA (*Pigr*$^{-/-}$) were examined using *Pigr*$^{+/-}$ males and females [7]. The pups of this mouse model could receive passive SIgA from their mothers during lactation but were unable to generate active SIgA in the intestine, allowing them to establish normal intestinal microbiota at weaning [7]. After the weaning process, the fecal SIgA levels in the *Pigr*$^{-/-}$ mice decreased dramatically, suggesting that the active production of intestinal SIgA was minimal (Figure 3G). As with the wild-type (WT) mice, the 30 d LDP *Pigr*$^{-/-}$ mice showed different mucosal bacterial compositions, as well as reduced levels of SFB and *Lactobacillus,* compared to Ctr mice (Figure 3H). FMT restored both the SFB and *Lactobacillus,* while probiotics could only restore the *Lactobacillus* (Figure 3I). However, the transient LDP treatment-induced alteration of the intestinal microbiota was not persistent, as observed in the WT mice. No significant differences were evident among the mucosal bacterial compositions in any of the treatments of the 25-week-old *Pigr*$^{-/-}$ mice (Figure 3I).

Finally, since the B cells in the intestine produce intestinal IgA, we then sought to determine whether LDP-induced changes to the B cells were responsible for the prolonged modifications of GM. Therefore, pan B cells (including plasma cells) derived from LDP-treated or LDP–free intestines pooled from the ileum, colon, Peyer's patches, and mesenteric lymph nodes, were transferred into B cell-deficient (μMt) mice. Twelve weeks after the transfer, the microbial ileal mucosal samples were collected and analyzed. As expected, after the transfer, all μMt mice had B cell-generated IgA in their intestines, even though no significant differences were evident in the SIgA levels of these mice (Figure 3J). However, the bacterial composition of the ileal mucosa samples of LDPR was different compared to that of CtrR and FR, suggesting that the LDP-induced alteration of the intestinal B cell pools mediated the long-term changes in the intestinal microbiota (Figure 3K).

Collectively, these results indicated that the early-lifetime disturbance of microbiota resulted in a long-term effect on the IgA responses, leading to long-lasting dysbiosis.

Dysbiosis resulted in MetS

Since intestinal microbiota is closely linked to metabolism, we examined the influence of LDP on the metabolism and its correlation with microbiota and IgA. We firstly evaluated the changes in metabolism in the 30-day-old mice. LDP decreased the serum levels of peptide YY (PYY), an anti-obesity peptide secreted by L cells in the gastrointestinal tract [24] (Figure 4D). Contrarily, insulin-like growth factor-1 (IGF-1), which has been shown to promote growth and preadipocyte proliferation and is linked to obesity [25-28], was increased in LDP mice (Figure 4E). Interestingly, insulin, which is structurally and functionally related to IGF-1 [28], was also present in higher concentrations in the LDP mice (Figure 4F). FMT significantly reversed the LDP-induced disturbance in these serum hormones, while probiotics could only moderately accomplish the same task (Figures D, E, and F).

RNA-sequencing identified 453 differentially expressed genes in the livers of the LDP and Ctr mice, of which 263 genes (58.7%) were concurrently affected by LDP and FMT (Figures 4H and 4J). Notably, 258

of these 263 genes (approximately 100%) had more comparable expression levels to Ctr mice in F mice than to those in LDP mice, suggesting the effective restoration of the LDP-induced disturbance in the hepatic gene expression by FMT (Figure 4I). The LDP mice exhibited significantly (padj < 0.05, |z-sore| > 2) influenced biological functions related to microbiota or immunity, such as dendritic cell maturation, GM-CSF signaling, and the role of pattern recognition receptors in recognition of bacteria and viruses [29, 30] (Figure S4E). FMT treatment either fully or partially restored most of these functions, especially those related to the responses to microbiota (Figure S4E). Contrary to FMT, probiotics had a much weaker influence on the restoration of the LDP-induced disturbance of the hepatic metabolism (Figures 4H to 4I and S4E), which corresponded with the moderate improvement in the intestinal microbiota of probiotic-treated mice.

Next, the long-term influence on the metabolism of 25-week-old WT mice was determined. A decrease in the PYY and an increase in IGF-1 and insulin were also observed in 25-week-old LDP mice, who also exhibited increased serum leptin, glucose, and triglyceride levels (Figures 4G, S4B and S4C). Furthermore, the LDP mice displayed higher hepatic steatosis and triglyceride levels, as well as increased lipid deposition in the adipose tissues (Figures S4F–S4G and S5A–S5C). The body weight and fat mass in the 25-week-old LDP mice were also elevated compared to that of the Ctr mice (Figures 4A and 4B). The LDP-induced MetS were completely inhibited by FMT but only displayed moderate improvement when exposed to probiotics, which was consistent with the results obtained from intestinal microbiota (Figures 4, S4, and S5).

The metabolic changes in the conventionalized GF mice produced similar results than their donors (Figures 4K–4O). The examination of the 10-week-old LDPR mice showed increases in body weight and fat mass, as well as serum IGF-1, insulin, leptin, and glucose levels compared to the Ctr mice, which were fully restored in FR but only partially in PR mice (Figures 4K–4O).

Finally, metabolic changes in the 25-week-old *Pigr*$^{-/-}$ mice were investigated to determine the role of SIgA in LDP-induced MetS (Figures S5D–S5J). As with the results obtained for intestinal microbiota, no significant differences were evident in the body weight, fat mass, serum hormones, glucose and triglyceride levels, or the hepatic triglyceride in any of the treatments (Figures S5D–S5H). Furthermore, the lipid deposition of adipose tissues was also comparable between the LDP-free and LDP-treated mice (Figures S5I and S5J).

Therefore, when the intestinal microbiota was disturbed, the metabolism of the mice was influenced, indicating that dysbiosis induced by the LDP treatment caused MetS in the mice.

Discussion

In this study, we showed that the transient LDP treatment of newborn mice reduced the abundance of SFB and *Lactobacillus*, decreased the SIgA level, and disturbed GM, eventually causing MetS. The LDP-induced dysbiosis resulted in the long-lasting dysfunction of IgA responses, which mediated the long-

term effects of early-lifetime LDP treatment on microbiota and metabolism. The restoration of the intestinal IgA levels via several FMT or probiotic administrations during the LDP treatment period fully (FMT) or partially (probiotics) prevented LDP-induced MetS.

The small intestine is the primary location for IgA production, and the results revealed a more profound influence of LDP on the bacterial composition in the ileal mucosa. Two dominant bacteria during early-lifetime period, namely SFB and *Lactobacillus*, and known to be sensitive to penicillin [31, 32], were reduced upon LDP treatment. FMT restored both the abundance of SFB and *Lactobacillus*, while probiotic treatment only restored *Lactobacillus*. SFB is well-known for inducing the differentiation and maturation of Th17 cells, which are implicated in coordinating IgA responses [33], while robust IgA responses induced by SFB was also observed [34]. In line with this, we found decreased SIgA levels in the LDP mice. In addition to SFB, *Lactobacillus* also induced IgA production but with a weaker effect [35], which may explain the discrepancy between FMT and probiotic treatment on the restoration of IgA production. Plasma cells secreting bacteria-specific IgA in the gut propria can survive and secrete IgA for prolonged periods of time [36]. A transient flagellin treatment elicited an elevation in the fecal and systemic IgA levels for at least three months [11]. In accord, we found that the differences of intestinal SIgA levels of the LDP and Ctr mice existed at the end of the experiment, as well as between the LDP and the F and P mice. Notably, the treatment time is important for the duration of microbiota-induced IgA responses, since the intestinal IgA reduction continued until the end of the experiment (25 weeks) in the WT SPF mice (whose GM was disturbed since birth) but disappeared in conventionalized GF mice (received GM at 30 d old) 12 weeks after the GM transfer.

The immune exclusion of possible pathogenic antigens (such as bacteria and food) and the promotion of commensal colonization, especially rare bacteria, of IgA contribute to the variety and homeostasis of GM [37]. It has been shown that a lack of SIgA in breast milk during lactation had a lifelong influence on the fecal bacterial composition of mice [7]; while our results indicated that a decrease in the intestinally active SIgA produced by pups only had a persistent impact on mucosal GM, not luminal GM. This finding may be attributed to the mucosal GM being more stable and less susceptible to environmental factors than luminal GM. The immunization of mice with flagellin derived from *Salmonella*, belonging to the phylum Proteobacteria, elicited the increased production of intestinal and serum IgA targeting flagellated bacteria and the decreased abundance of Proteobacteria while protecting the mice from HFD-induced obesity [11]. Similar to this, we found that LDP-induced reduction in SFB and *Lactobacillus*, both belonging to the phylum Firmicutes, caused the expansion of Firmicutes in LDP mice. Furthermore, it is worth noting that because of the specialty of IgA and similarities in the surface epitopes of intestinal bacteria, the IgA induced by a specific bacteria may target a variety of microbes, as shown by the results of this and other studies [11, 38]. FMT and probiotic treatments restored the *Lactobacillus* to a comparable level while SFB only recovered slightly when exposed to probiotics, which may cause differences in the production and specialty of the IgA in the two treatments, thereby contributing to the observed discrepancies.

In addition, FMT and probiotics are both effective interventions to improve LDP-induced MetS. Although FMT is more efficient than probiotics, finding proper donors, as well as the acceptability and safety (especially for infants), are significant issues that need to be addressed. Probiotics are safer and more acceptable than FMT but exhibit lower efficiency. Additionally, the initiation and duration times, as well as the dosage level and frequency, are factors that should be considered. Moreover, future studies should focus on the differences between FMT and probiotics (such as the efficiency of SFB restoration in mice) and seek efficient and safe ways to treat Abx-induced MetS.

Conclusions

Transient LDP treatment on newborn mice disturbed the GM, mainly the reduction in penicillin-sensitive bacteria SFB and Lactobacillus. The reduction of these two IgA-inducing bacteria, as well as the dysbiosis, resulted in the permanent disturbance of intestinal immunity, mainly IgA response to microbes. The disturbance of IgA response leads to long-term dysbiosis and MetS, including adiposity, hepatic steatosis and impaired glucose metabolism.

Methods

Animals

Wild-type specific pathogen free animals

Wild-type (WT) C56BL/6J mice purchased at 8 weeks of age (Vital River Laboratory Animal Technology. Co., Ltd., China) were randomly paired (1:1) after adapting for one week and fed a standard diet (#12450B, Research Diets, Inc.). After cohousing for 4 days (one estrous cycle for house mouse), females were separated from the males and fed solely. During and after cohousing, pregnancies and due dates were monitored and calculated according to the formation of vaginal plugs and body weight changes, respectively.

Pups (and their mothers) were randomly assigned to four groups: (1) low-dose penicillin (LDP)-free control group (Ctr) that received no antibiotics, (2) LDP-treated control group (LDP) that received antibiotics only, (3) FMT-treated group (F) that received LDP and fecal microbiota transplantation treatments, and (4) probiotics-treated group (P) that received LDP and probiotic cocktail treatments. Pups were separated from their mothers at 21 days. Pups in every group were from at least three dams and born within 24 hours. Pups in the Ctr and F groups were born within 24 hours. For the LDP, F and P groups, dams received antibiotics at a dose of 10 mg/L to deliver approximately 1.5 mg per kg body weight about one week prior to birth and were continuously maintained on penicillin. Pups in the three groups were exposed to penicillin until 30 days of age either through their mother or through drinking water. After the LDP treatment, pups were divided by sexes and kept 2~3/cages. Pups in the F and P groups were gavaged with fecal microbiota from Ctr and probiotics, respectively at 12, 16, 20, 24 and 28 days of age. For the FMT group, feces were collected from pups in the Ctr group and immediately placed

in prereduced anaerobically sterilized PBS, pooled under anaerobic conditions, settled with gravity for 2 minutes, and then the supernatant was transferred to pups in the F group. For the P group, pups were gavaged with prereduced anaerobically sterilized PBS containing *Lactobacillus bulgaricus* and *Lactobacillus rhamnosus* GG at ~10^8/mL for each bacterium. For the Ctr and LDP groups, pups were gavaged with prereduced anaerobically sterilized PBS on the same days. For 12 day and 16 day mice, 50 μL and 100 μL liquid were gavaged, respectively; for the rest, 150 μL was gavaged. All pups were fed on normal diet (#D12450B, Research Diets, Inc.) and allowed *ad libitum* access to food and water.

Germ-free animals

For the microbiota transfer to germ-free (GF) animals experiment, feces were collected from 30-day-old donors from each group and immediately placed in prereduced anaerobically sterilized PBS, homogenized under anaerobic conditions, settled with gravity for 2 minutes, and then the supernatant was transferred to even-aged GF C57BL/6 mice (n = 8 for each group, n (females) = n (males) = 4). After transfer, the conventionalized GF mice were housed in standard SPF conditions, and food and water were provided *ad libitum*.

SIgA-deficient mice

It is known that SIgA-deficient mice have a different gut microbiota (GM) compared to WT mice. Therefore to ensure a comparable GM was obtained by SIgA-deficient pups to WT during birth and nursing, *Pigr*+/- males and females, which can produce normal SIgA and therefore have similar GM to WT mice[7], were used to generate SIgA-deficient pups. Specifically, 8-week-old $Pigr^{+/-}$ females and males were mated as above specified, genotypes of pups were identified at 10 days of age and only $Pigr^{-/-}$ female pups were chosen for the following experiment as specified above.

B cell-deficient (μMT) mice

Separation and transfer of pan B cells to B cell-deficient (μMT) mice was conducted as previously described with some modification [39]. Pan B cells (includes plasma cells) from the spleens, Peyer's patches, mesenteric lymph nodes and ileal and colonic lamina propria of 30 day LDP-treated or -free WT SPF mice were purified using negative selection (>90% purity, EasySep; StemCell Technologies) and injected intraperitoneally (~5.5×10^6 cells) in even-aged μMT mice.

Animal management and sampling

Mice were housed in standard specific pathogen-free (SPF) conditions (12/12-hour light-dark cycle, humidity at 50 ± 15%, temperature of 22 ± 2°C), and food and water were provided *ad libitum*. The food used in this study was sterilized using radiation (25.0 kGy). Food intake was recorded every week. Body weight was recorded weekly. At the end of the experimental period, the mice were fasted for 12 hours, and plasma was collected by eyeball extirpation. The lumen contents of the distal ileum and proximal colon were collected by washing the lumen with sterilized PBS, and the mucosal samples were collected by

scraping the intestinal wall with sterilized glass slides. Then, the samples were stored at -80°C for microbial analysis. The contents of the cecum were collected and stored at -80°C for the analysis of secreted IgA (SIgA). The weights of the liver, inguinal white adipose tissue (iWAT), epididymal white adipose tissue (eWAT) and mesenteric white adipose tissue (mWAT) were measured. Tissues were preserved at -80°C for gene expression analysis (for ileum, all fat and mesentery were removed, and Peyer's patches were excised from the ileum), and the liver, iWAT, colon and ileum were fixed using 4% paraformaldehyde and used for hematoxylin-eosin (H&E) staining, immunofluorescence and immunohistochemistry analysis.

Derivation of "pure or none Fimicutes" animals

Wild-type C57BL/6 mice purchased at 4 weeks of age (Vital River Laboratory Animal Technology. Co., Ltd., China) were randomly assigned to 3 groups (n = 3 for each group) after adapting for 2 weeks: (1) "pure Firmicutes" group 1 that fed a HFD (60% energy from fat, #D12492, Research Diets, Inc.), (2) "pure Firmicutes" group 2 that fed a standard diet with 0.5 g/L vancomycin and streptomycin in their drinking water, and (3) "none Firmicutes" group that fed a standard diet with 1g/L norfloxacin and 0.5g/L cefotaxime in their drinking water. All mice were maintained in a standard SPF environment as specified above, and food and water (with 4g/L sucralose) were provided *ad libitum*. After 4 weeks experiment, mice were killed and cecal contents were collected and stored at -80°C for further analysis.

The guidelines of the institute regarding the care and use of laboratory animals were followed. This study was approved by the Animal Experiment Committee of the College of Food Science and Nutritional Engineering at China Agricultural University.

Ileum tissue culture

Mouse ileum was obtained and cultured as previously described with some modification [40]. Distal ileum samples were washed and cultured using RPMI 1640 supplemented with 10% FCS and penicillin/streptomycin 50 mg/ml at 37°C and 5% CO2 in 24-well plates. Two ileum samples per well (~ 3 mm) were cultured for each group (n = 4). Two days after co-culture with antigens, culture medium was collected and supernatants were centrifuged and stored at -80°C for the analysis of IgA and cells were collected for the analysis gene expression.

Quantitative Real-time PCR (qPCR) Analysis

Total RNA was extracted using TRIzol^{TM} reagent (Invitrogen) according to the manufacturer's instructions. Reverse transcription of the total RNA (2.5 μg) was performed with a high-capacity cDNA reverse transcription kit (Promega Biotech Co., Ltd). qPCR was run in triplicate for each sample and analyzed in a LightCycler 480 real-time PCR system (Roche). Data were normalized to the internal control *β-actin* and analyzed using the △△CT method. The expression of genes in iWAT, the liver, ileum and

colon, as well as the bacterial and fungal load, were determined through qPCR (the related genes and primers used are shown in Table S1).

Quantification of the bacterial and fungal loads through qPCR was conducted as previously described[41]. Briefly, the total bacterial DNA was isolated from the samples with a QIAamp DNA Stool Mini Kit (Qiagen) following the manufacturer's instructions. For the isolation of fungal DNA, samples were suspended in 50 mM Tris buffer (pH 7.5) supplemented with 1 mM EDTA, 0.2% b-mercaptoethanol and 1000 units/ml of lyticase (Sigma), incubated at 37°C for 30 min to disrupt fungal cells as described[42], prior to processing through the QIAamp DNA Stool Mini Kit (Qiagen). The DNA was then subjected to qPCR using a QuantiFast SYBR Green PCR kit (Bio-Rad) with specific primers (Table S1).

Determination of Body Composition through MRI

MRI experiments were performed on 30-day-old and 25-week-old mice. The body composition was determined using MesoQMR instrument (Testniumag, Shanghai, China) with a 60 mm receiver and 0.5 ± 0.08 T magnetic field strength. To obtain high resolution scanned MRI images, MRI measurements were performed on a 7.0 T Varian MRI instrument (Varian Medical Systems, Palo Alto, CA, USA) using a 40 mm volume and receiver coil at the Institute of Laboratory Animal Sciences, Chinese Academy of Medical Sciences. Prior to the experiments, the mice were initially anesthetized with 2% isoflurane in a dedicated chamber. During the course of MRI, anesthesia levels were reduced to 1.5–1% in a combination of medical air and medical oxygen. The mice were positioned in the prone position, and respiratory-gated image acquisition was performed. MRI images of the mice were analyzed by Argus software.

Plasma Biochemical Parameters

The plasma biochemical parameters, including, glucose, cholesterol and triglyceride (TG) levels, were determined by a 3100 Clinical Analyzer (Hitachi High-Technologies Corporation, Japan).

Quantification of Serum Hormones and SIgA

Serum hormones including leptin, insulin, PYY, GLP-1, IGF-1 and GIP, as well as total caecal SIgA levels were determined using ELISA kits (Sangon Biotech, Shanghai, China) according to the manufacturer's recommendations.

Separation of antigens and determination of IgA to the specific antigens were conducted as described with some modification[8, 11]. Briefly, to prepare antigens from cecal contents of mice carrying GM composed of "pure or none Firmicutes", cecal contents of mice from each group were normalized by bacterial loads (determined by qPCR as previously described[19]), pooled (n = 3) in PBS (sterilized with a 0.22 μm filter), vortexed for 5 min, and centrifuged for 5 min at 13000 RPM, 4°C. Samples were then sonicated for 15 min and centrifuged for 15 min at 13000 RPM, 4°C. Supernatant was taken and protein

was measured using BCA assay (Thermo Fisher). For the determination of IgA to specific antigens, 96-well microtiter plates (Costar, Corning, New York) were coated with 1 mg/ml of antigen in 9.6 pH bicarbonate buffer overnight at 4 °C, then IgA from the cecal contents of 30 day or 25 week mice were loaded at 1:20 dilution for 1 h at 37°C. Anti-IgA Biotin and HRP Conjugated Streptavidin were used to detect binding of IgA.

Immunofluorescence

Immunofluorescence for immunoglobulin A was conducted using FITC-conjugated secondary antibody at a 1:500 dilution and applied to the section for 2 h. Observations and analyses were performed with a Zeiss LSM 700 confocal microscope.

Histology

Tissues fixed in 4% paraformaldehyde were cut into 5 μm sections after being embedded in paraffin. Multiple sections were prepared and stained with hematoxylin and eosin (H&E) for general morphological observation.

GM Analysis

The microbial community of fecal, mucosal and lumen samples of colon and ileum were analyzed through the sequence of 16S rRNA gene V4 region. Briefly, Total genome DNA from samples was extracted using CTAB/SDS method. DNA concentration and purity was monitored on 1% agarose gels. According to the concentration, DNA was diluted to 1 ng/μL using sterile water. 16S rRNA gene V4 region were amplified used specific primer for V4 region (515F-806R) with the barcode. All PCR reactions were carried out in 30 μL reactions with 15 μL of Phusion® High-Fidelity PCR Master Mix (New England Biolabs); 0.2 μM of forward and reverse primers, and about 10 ng template DNA. Thermal cycling consisted of initial denaturation at 98°C for 1 min, followed by 30 cycles of denaturation at 98°C for 10 s, annealing at 50°C for 30 s, and elongation at 72°C for 30 s. Finally 72°C for 5 min. Mix same volume of 1×loading buffer (contained SYB green) with PCR products and operate electrophoresis on 2% agarose gel for detection. PCR products were mixed in equidensity ratios. Then, mixture PCR products were purified with GeneJETTM Gel Extraction Kit (Thermo Scientific). Sequencing libraries were generated using Ion Plus Fragment Library Kit 48 rxns (Thermo Scientific) following manufacturer's recommendations. The library quality was assessed on the Qubit@2.0 Fluorometer (Thermo Scientific). At last, the library was sequenced on an Ion S5TM XL platform and 400 bp/600 bp single-end reads were generated.

Single-end reads was assigned to samples based on their unique barcode and truncated by cutting off the barcode and primer sequence. Quality filtering on the raw reads was performed under specific filtering conditions to obtain the high-quality clean reads according to the Cutadapt (V1.9.1,

http://cutadapt.readthedocs.io/en/stable/) quality controlled process. The reads were compared with the reference database (Silva database, https://www.arb-silva.de/) using UCHIME algorithm (UCHIME Algorithm, http://www.drive5.com/usearch/manual/uchime_algo.html) to detect chimera sequences, and then the chimera sequences were removed[43]. Then the Clean Reads finally obtained.

Alpha diversity is applied in analyzing complexity of species diversity for a sample through 6 indices, including Observed-species, Chao1, Shannon, Simpson, ACE, Good-coverage. All this indices in our samples were calculated with QIIME (V1.7.0) and displayed with R software (V2.15.3). Beta diversity analysis was used to evaluate differences of samples in species complexity, Beta diversity on both weighted and unweighted unifrac was calculated by QIIME software (V1.7.0). Principal Coordinate Analysis (PCoA) was performed to get principal coordinates and visualize from complex, multidimensional data. A distance matrix of weighted or unweighted unifrac among samples obtained before was transformed to a new set of orthogonal axes, by which the maximum variation factor is demonstrated by first principal coordinate, and the second maximum one by the second principal coordinate, and so on. PCoA analysis was displayed by WGCNA package, stat packages and ggplot2 package in R software (V2.15.3).

RNA-sequencing

Total RNA of the liver and ileum were extracted using TRIzol^{TM} reagent (Invitrogen) according to the manufacturer's instructions. RNA degradation and contamination was monitored on 1% agarose gels; RNA purity was checked using the NanoPhotometer® spectrophotometer (IMPLEN, CA, USA); RNA concentration was measured using Qubit® RNA Assay Kit in Qubit®2.0 Flurometer (Life Technologies, CA, USA); RNA integrity was assessed using the RNA Nano 6000 Assay Kit of the Bioanalyzer 2100 system (Agilent Technologies, CA, USA). Then a total amount of 3 μg RNA per sample was used as input material for the RNA sample preparations. Sequencing libraries were generated using NEBNext® UltraTM RNA Library Prep Kit for Illumina® (NEB, USA) following manufacturer's recommendations and index codes were added to attribute sequences to each sample. Briefly, mRNA was purified from total RNA using poly-T oligo-attached magnetic beads. Fragmentation was carried out using divalent cations under elevated temperature in NEBNext First Strand Synthesis Reaction Buffer (5X). First strand cDNA was synthesized using random hexamer primer and M-MuLV Reverse Transcriptase (RNase H^-). Second strand cDNA synthesis was subsequently performed using DNA Polymerase I and RNase H. Remaining overhangs were converted into blunt ends via exonuclease/polymerase activities. After adenylation of 3' ends of DNA fragments, NEBNext Adaptor with hairpin loop structure were ligated to prepare for hybridization. In order to select cDNA fragments of preferentially 250~300 bp in length, the library fragments were purified with AMPure XP system (Beckman Coulter, Beverly, USA). Then 3 μL USER Enzyme (NEB, USA) was used with size-selected, adaptor-ligated cDNA at 37°C for 15 min followed by 5 min at 95°C before PCR. Then PCR was performed with Phusion High-Fidelity DNA polymerase, Universal PCR primers and Index (X) Primer. At last, PCR products were purified (AMPure XP system) and library quality was assessed on the Agilent Bioanalyzer 2100 system. The clustering of the index-coded samples

was performed on a cBot Cluster Generation System using TruSeq PE Cluster Kit v3-cBot-HS (Illumia) according to the manufacturer's instructions. After cluster generation, the library preparations were sequenced on an Illumina Hiseq platform and 125 bp/150 bp paired-end reads were generated.

Raw data (raw reads) of fastq format were firstly processed through in-house perl scripts. In this step, clean data (clean reads) were obtained by removing reads containing adapter, reads containing ploy-N and low quality reads from raw data. At the same time, Q20, Q30 and GC content the clean data were calculated. All the downstream analyses were based on the clean data with high quality. Reference genome and gene model annotation files were downloaded from genome website directly. Index of the reference genome was built using Hisat2 (V2.0.5) and paired-end clean reads were aligned to the reference genome using Hisat2. We selected Hisat2 as the mapping tool for that Hisat2 can generate a database of splice junctions based on the gene model annotation file and thus a better mapping result than other non-splice mapping tools. featureCounts (V1.5.0-p3) was used to count the reads numbers mapped to each gene. And then FPKM of each gene was calculated based on the length of the gene and reads count mapped to this gene. FPKM, expected number of Fragments Per Kilobase of transcript sequence per Millions base pairs sequenced, considers the effect of sequencing depth and gene length for the reads count at the same time, and is currently the most commonly used method for estimating gene expression levels. Differential expression analysis of two conditions/groups (two biological replicates per condition) was performed using the DESeq2 R package (V1.16.1). DESeq2 provide statistical routines for determining differential expression in digital gene expression data using a model based on the negative binomial distribution. The resulting P-values were adjusted using the Benjamini and Hochberg's approach for controlling the false discovery rate. Genes with an adjusted P-value <0.05 found by DESeq2 were assigned as differentially expressed. Prior to differential gene expression analysis, for each sequenced library, the read counts were adjusted by edgeR program package through one scaling normalized factor. Differential expression analysis of two conditions was performed using the edgeR R package (V3.18.1). The P values were adjusted using the Benjamini & Hochberg method. Corrected P-value of 0.05 and $|\log_2 \text{foldchange}| > 1.2$ was set as the threshold for significantly differential expression.

Statistical Analysis

All data reported in this paper are expressed as the means ± SEMs. The data were evaluated by one-way ANOVA, Wilcox, or Mann-Whitney U tests. All statistics were analyzed by SPSS software, and all analyses were performed with GraphPad Prism 7.

Supplementary Information

Additional file 1: Table S1. Primers used in this study. **Table S2**. Key resources table.

Additional file 2: Figure S1. Effects of the LDP treatment on microniota. **Figure S2**. The relative abundances of bacteria at phylum and genus level. **Figure S3**. The long-term effects of LDP on intestinal

microbiota. **Figure S4**. Changes in the metabolism of mice. **Figure S5.** Changes of the serum hormones and adipose tissue.

Declarations

Ethics approval and consent to participate

Not applicable.

Consent for publication

Not applicable.

Availability of data and materials

The RNA-seq and 16S rRNA gene sequencing data supporting this research are available on NCBI with accession number PRJNA577425 (review link: https://dataview.ncbi.nlm.nih.gov/object/PRJNA577425?reviewer=n781bce0r0aliiectnhc39kfs5). All other data that support the findings of this study are available from the corresponding author upon reasonable request.

Competing interests

The authors declare no competing interests.

Funding

The work was supported by the Research on Blueberry Functional Ingredients and the Development of New Blueberry Wine (201805410611582).

Author contributions

J.Z. and J.G. designed the study and wrote the manuscript. J.G. and X.H. performed the experiments. Y.Y. and W.H. contributed to the data analysis.

Acknowledgements

Not applicable.

References

1. Cox LM, Blaser MJ. Antibiotics in early life and obesity. Nat Rev Endocrinol. 2015;11(3):182–90.
2. Tamburini S, Shen N, Wu HC, Clemente JC. The microbiome in early life: implications for health outcomes. Nat Med. 2016;22(7):713–22.

3. Cox LM, Yamanishi S, Sohn J, Alekseyenko AV, Leung JM, Cho I, Kim SG, Li H, Gao Z, Mahana D, et al. Altering the intestinal microbiota during a critical developmental window has lasting metabolic consequences. Cell. 2014;158(4):705–21.
4. Cho I, Yamanishi S, Cox L, Methe BA, Zavadil J, Li K, Gao Z, Mahana D, Raju K, Teitler I, et al. Antibiotics in early life alter the murine colonic microbiome and adiposity. Nature. 2012;488(7413):621–6.
5. Knoop KA, Gustafsson JK, McDonald KG, Kulkarni DH, Coughlin PE, McCrate S, Kim D, Hsieh C-S, Hogan SP, Elson CO. Microbial antigen encounter during a preweaning interval is critical for tolerance to gut bacteria. Science immunology. 2017;2(18):eaao1314.
6. Koren O, Goodrich JK, Cullender TC, Spor A, Laitinen K, Bäckhed HK, Gonzalez A, Werner JJ, Angenent LT, Knight R. Host remodeling of the gut microbiome and metabolic changes during pregnancy. Cell. 2012;150(3):470–80.
7. Rogier EW, Frantz AL, Bruno ME, Wedlund L, Cohen DA, Stromberg AJ, Kaetzel CS: **Secretory antibodies in breast milk promote long-term intestinal homeostasis by regulating the gut microbiota and host gene expression**. *Proceedings of the National Academy of Sciences* 2014, **111**(8):3074–3079.
8. Mirpuri J, Raetz M, Sturge CR, Wilhelm CL, Benson A, Savani RC, Hooper LV, Yarovinsky F. Proteobacteria-specific IgA regulates maturation of the intestinal microbiota. Gut Microbes. 2014;5(1):28–39.
9. Saari A, Virta LJ, Sankilampi U, Dunkel L, Saxen H. Antibiotic exposure in infancy and risk of being overweight in the first 24 months of life. Pediatrics. 2015;135(4):617–26.
10. Risnes KR, Belanger K, Murk W, Bracken MB: **Antibiotic exposure by 6 months and asthma and allergy at 6 years**: **findings in a cohort of 1,401 US children**. *American journal of epidemiology* 2011, **173**(3):310–318.
11. Tran HQ, Ley RE, Gewirtz AT, Chassaing B. Flagellin-elicited adaptive immunity suppresses flagellated microbiota and vaccinates against chronic inflammatory diseases. Nat Commun. 2019;10(1):5650.
12. Vijay-Kumar M, Aitken JD, Carvalho FA, Cullender TC, Mwangi S, Srinivasan S, Sitaraman SV, Knight R, Ley RE, Gewirtz AT. Metabolic syndrome and altered gut microbiota in mice lacking Toll-like receptor 5. Science. 2010;328(5975):228–31.
13. Pabst O. New concepts in the generation and functions of IgA. Nat Rev Immunol. 2012;12(12):821–32.
14. Kubinak JL, Round JL. Do antibodies select a healthy microbiota? Nat Rev Immunol. 2016;16(12):767–74.
15. Macpherson AJ, Koller Y, McCoy KD. The bilateral responsiveness between intestinal microbes and IgA. Trends Immunol. 2015;36(8):460–70.
16. Bunker JJ, Flynn TM, Koval JC, Shaw DG, Meisel M, McDonald BD, Ishizuka IE, Dent AL, Wilson PC, Jabri B. Innate and adaptive humoral responses coat distinct commensal bacteria with immunoglobulin A. Immunity. 2015;43(3):541–53.

17. Donaldson G, Ladinsky M, Yu K, Sanders J, Yoo B, Chou W-C, Conner M, Earl A, Knight R, Bjorkman P. Gut microbiota utilize immunoglobulin A for mucosal colonization. Science. 2018;360(6390):795–800.
18. Gutzeit C, Magri G, Cerutti A. Intestinal IgA production and its role in host-microbe interaction. Immunological reviews. 2014;260(1):76–85.
19. Guo JL, Han X, Zhan JC, You YL, Huang WD. Vanillin Alleviates High Fat Diet-Induced Obesity and Improves the Gut Microbiota Composition. Frontiers In Microbiology. 2018;9:2733.
20. Wang Y, Liu L, Moore DJ, Shen X, Peek R, Acra SA, Li H, Ren X, Polk DB, Yan F. An LGG-derived protein promotes IgA production through upregulation of APRIL expression in intestinal epithelial cells. Mucosal immunology. 2017;10(2):373–84.
21. Lecuyer E, Rakotobe S, Lengline-Garnier H, Lebreton C, Picard M, Juste C, Fritzen R, Eberl G, McCoy KD, Macpherson AJ, et al. Segmented filamentous bacterium uses secondary and tertiary lymphoid tissues to induce gut IgA and specific T helper 17 cell responses. Immunity. 2014;40(4):608–20.
22. Bunker JJ, Bendelac A. IgA Responses to Microbiota. Immunity. 2018;49(2):211–24.
23. Bunker JJ, Erickson SA, Flynn TM, Henry C, Koval JC, Meisel M, Jabri B, Antonopoulos DA, Wilson PC, Bendelac A. **Natural polyreactive IgA antibodies coat the intestinal microbiota**. *Science* 2017, 358(6361).
24. Batterham RL, Heffron H, Kapoor S, Chivers JE, Chandarana K, Herzog H, Le Roux CW, Thomas EL, Bell JD, Withers DJ. Critical role for peptide YY in protein-mediated satiation and body-weight regulation. Cell Metabol. 2006;4(3):223–33.
25. Garten A, Schuster S, Kiess W. The insulin-like growth factors in adipogenesis and obesity. Endocrinology Metabolism Clinics. 2012;41(2):283–95.
26. Yan J, Herzog JW, Tsang K, Brennan CA, Bower MA, Garrett WS, Sartor BR, Aliprantis AO, Charles JF: **Gut microbiota induce IGF-1 and promote bone formation and growth**. *Proceedings of the National Academy of Sciences* 2016, **113**(47):E7554-E7563.
27. Doyle SL, Donohoe CL, Lysaght J, Reynolds JV: **Visceral obesity, metabolic syndrome, insulin resistance and cancer**. *Proceedings of the Nutrition Society* 2012, **71**(1):181–189.
28. Renehan AG, Frystyk J, Flyvbjerg A. Obesity and cancer risk: the role of the insulin–IGF axis. Trends in Endocrinology Metabolism. 2006;17(8):328–36.
29. Chu H, Mazmanian SK. Innate immune recognition of the microbiota promotes host-microbial symbiosis. Nature immunology. 2013;14(7):668.
30. Negishi H, Miki S, Sarashina H, Taguchi-Atarashi N, Nakajima A, Matsuki K, Endo N, Yanai H, Nishio J, Honda K: **Essential contribution of IRF3 to intestinal homeostasis and microbiota-mediated Tslp gene induction**. *Proceedings of the National Academy of Sciences* 2012, **109**(51):21016–21021.
31. Bayrock D, Thomas K, Ingledew W. Control of Lactobacillus contaminants in continuous fuel ethanol fermentations by constant or pulsed addition of penicillin G. Appl Microbiol Biotechnol. 2003;62(5–6):498–502.

32. Davis CP, Savage DC. Effect of penicillin on the succession, attachment, and morphology of segmented, filamentous microbes in the murine small bowel. Infect Immun. 1976;13(1):180–8.
33. Cong Y, Feng T, Fujihashi K, Schoeb TR, Elson CO: **A dominant, coordinated T regulatory cell-IgA response to the intestinal microbiota**. *Proceedings of the National Academy of Sciences* 2009, **106**(46):19256–19261.
34. Klaasen H, Van der Heijden P, Stok W, Poelma F, Koopman J, Van den Brink M, Bakker M, Eling W, Beynen A. Apathogenic, intestinal, segmented, filamentous bacteria stimulate the mucosal immune system of mice. Infect Immun. 1993;61(1):303–6.
35. Ohland CL, Macnaughton WK. Probiotic bacteria and intestinal epithelial barrier function. Am J Physiol Gastrointest Liver Physiol. 2010;298(6):G807–19.
36. Hapfelmeier S, Lawson MA, Slack E, Kirundi JK, Stoel M, Heikenwalder M, Cahenzli J, Velykoredko Y, Balmer ML, Endt K. Reversible microbial colonization of germ-free mice reveals the dynamics of IgA immune responses. Science. 2010;328(5986):1705–9.
37. Pabst O, Cerovic V, Hornef M. Secretory IgA in the Coordination of Establishment and Maintenance of the Microbiota. Trends Immunol. 2016;37(5):287–96.
38. Palm NW, de Zoete MR, Cullen TW, Barry NA, Stefanowski J, Hao L, Degnan PH, Hu J, Peter I, Zhang W, et al. Immunoglobulin A coating identifies colitogenic bacteria in inflammatory bowel disease. Cell. 2014;158(5):1000–10.
39. Luck H, Khan S, Kim JH, Copeland JK, Revelo XS, Tsai S, Chakraborty M, Cheng K, Chan YT, Nøhr MK. Gut-associated IgA + immune cells regulate obesity-related insulin resistance. Nature communications. 2019;10(1):1–17.
40. Mesin L, Di Niro R, Thompson KM, Lundin KE, Sollid LM. Long-lived plasma cells from human small intestine biopsies secrete immunoglobulins for many weeks in vitro. J Immunol. 2011;187(6):2867–74.
41. Jiang TT, Shao TY, Ang WXG, Kinder JM, Turner LH, Pham G, Whitt J, Alenghat T, Way SS. Commensal Fungi Recapitulate the Protective Benefits of Intestinal Bacteria. Cell Host Microbe. 2017;22(6):809–16 e804.
42. Iliev ID, Funari VA, Taylor KD, Nguyen Q, Reyes CN, Strom SP, Brown J, Becker CA, Fleshner PR, Dubinsky M. Interactions between commensal fungi and the C-type lectin receptor Dectin-1 influence colitis. Science. 2012;336(6086):1314–7.
43. Haas BJ, Gevers D, Earl AM, Feldgarden M, Ward DV, Giannoukos G, Ciulla D, Tabbaa D, Highlander SK, Sodergren E. Chimeric 16S rRNA sequence formation and detection in Sanger and 454-pyrosequenced PCR amplicons. Genome research. 2011;21(3):494–504.

Figures

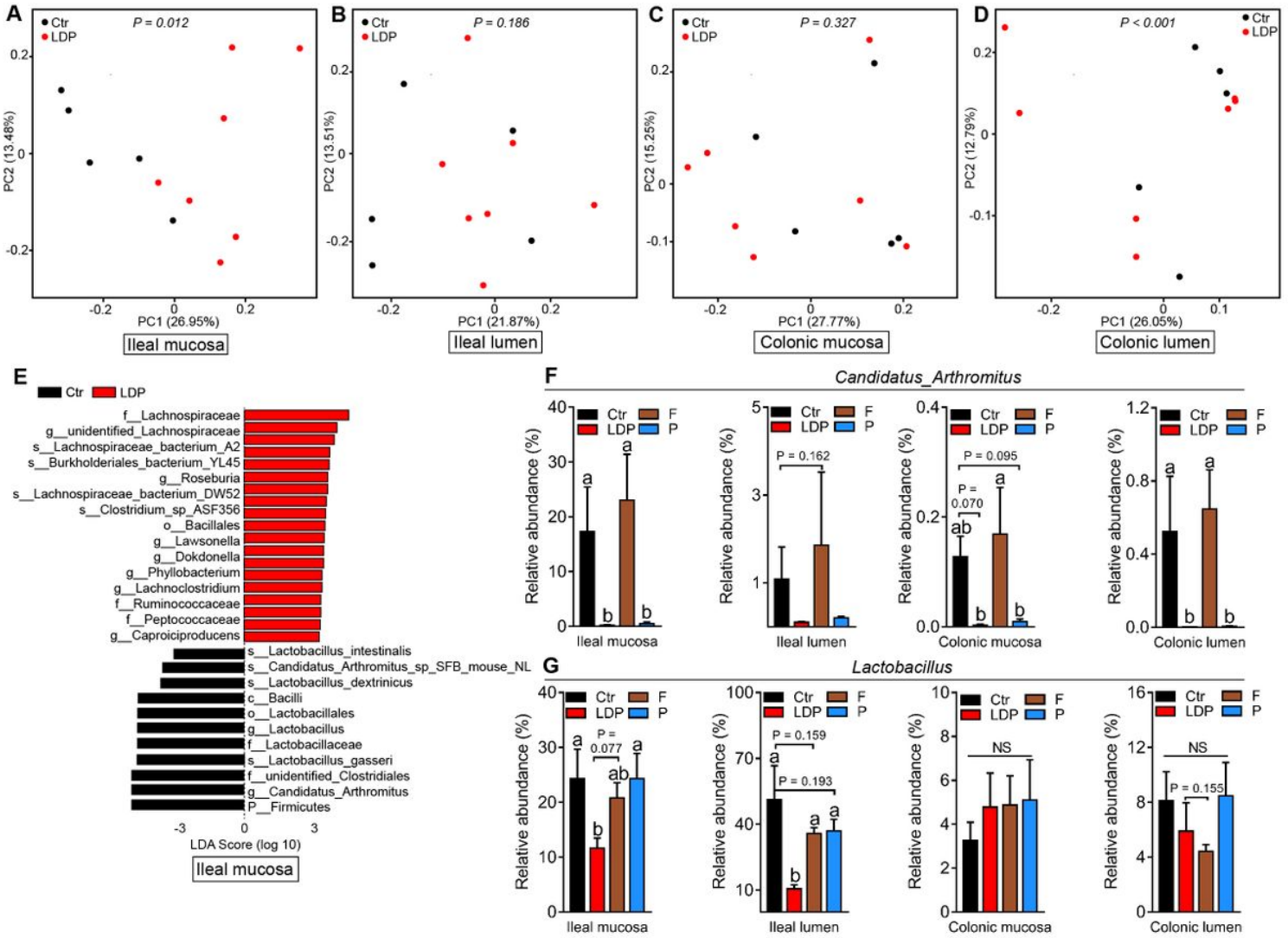

Figure 1

Microbiota disturbed by LDP-treatment. Study design: Some WT C57BL/6 mice were exposed to LDP (LDP, F, and P groups) several days before birth until 30 d old, while others were not (Ctr group). The mice were gavaged with sterilized pre-reduced PBS (Ctr and LDP groups), and fecal microbiota from the Ctr (F group) or probiotic (P group) groups at 4 d intervals from 12 d to 28 d of age. The mice in each group came from at least three dams, and pups with a bodyweight near the average level were selected for experiments before the first gavage. The pups were separated from dams at 21 d of age. For the analysis of the GM, the females and males were analyzed together since pups were kept together throughout the 30-day experiment. (A–D) The principal coordinate analysis (PCoA) based on the unweighted UniFrac distance indicated the differences in the bacterial composition between the LDP and the Ctr mice from different intestinal regions. Significance was determined using the Wilcox test. (E) Discrepant bacterial species identification of the ileal mucosa between the LDP and the Ctr mice was based on LEfSe analysis. (F and G) The relative abundance of Candidatus Arthromitus (F) and Lactobacillus (G) from the different intestinal regions, as determined by 16S rRNA gene sequencing. The F and P, mice treated with LDP while gavaged with microbiota from the Ctr (F) or probiotic (P) groups. Different letters indicate a

significant difference between the columns or points, $p < 0.05$, while NS indicates no significant difference. The LSD posthoc test or one-way ANOVA as compared to Dunnett's (T3). For all figures, n = 5 for the Ctr mice, n = 7 for the LDP mice, and n = 6 for the F and P mice.

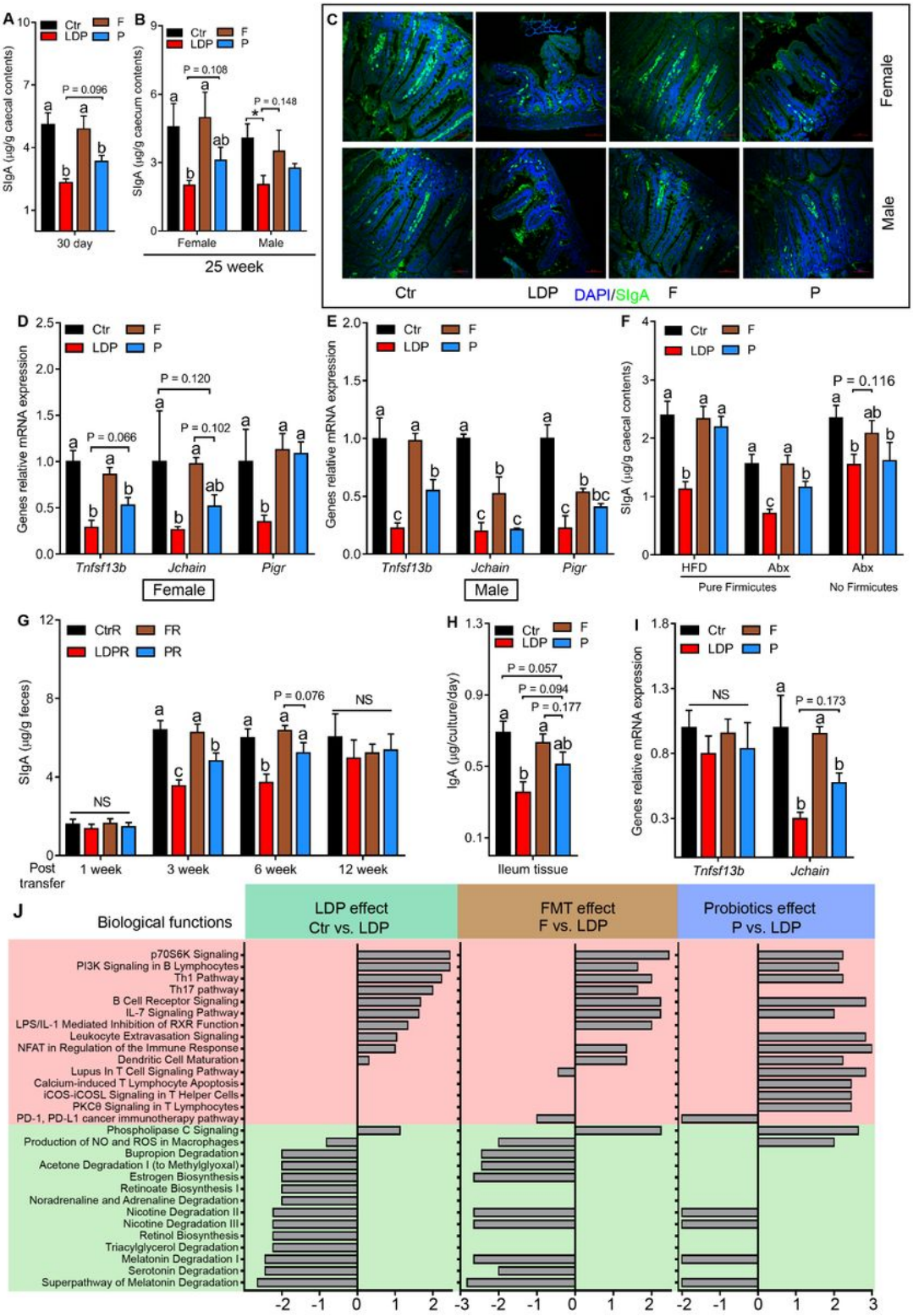

Figure 2

Changes in the microbiota-altered IgA production. (A) Caecal SIgA levels of the 30-d-old mice, where n = 5 for the Ctr mice, n = 7 for the LDP mice, and n = 6 for the F and P mice. (B) Caecal SIgA levels of the 25-

week-old mice. For A to G, n = 8 for the male and female Ctr mice and n = 9 for the male and female LDP mice. (C) Immunofluorescence assays targeting the SIgA of the distal ileum in the 30-d-old females (top) and males (bottom), respectively, where n = 2 for the female Ctr mice and n = 3 for the remaining groups of females and males. (D and E) The relative expression of genes related to the IgA production of ileum in the 30-d-old females (D) and males (E), where n = 2 for the female Ctr mice, n = 4 for the female LDP mice, and n = 3 for the remaining groups of females and males. (F) The caecal concentration of SIgA targeting “pure Firmicutes” induced by an HFD or Abx and targeting the “no Firmicutes” induced by Abx. (G) The fecal SIgA levels of the conventionalized GF mice transferred fecal microbiota from 30-d-old Ctr, LDP, F, and P mice, where n = 8 for all treatments. (H and I) IgA production (H) and relative gene expression (I) in the mouse ileum during in vitro cultivation with fecal microbiota derived from the Ctr, LDP, F, and P mice, n = 4. Four eight-week-old male SPF C57/BL6 mice were used for sampling. The ileum samples of each group were taken from all four mice and comprised the same intestinal regions. (J) Predicted canonical pathways that were represented differently ($P < 0.05$, $|z\text{-score}| > 2$), based on Ingenuity Pathway Analysis of the RNA-sequencing of ileal gene expression. For all figures, except C and J, different letters indicate a significant difference between columns or points, $p < 0.05$, and NS denotes no significant difference; LSD post hoc test or one-way ANOVA as compared to Dunnett’s test (T3).

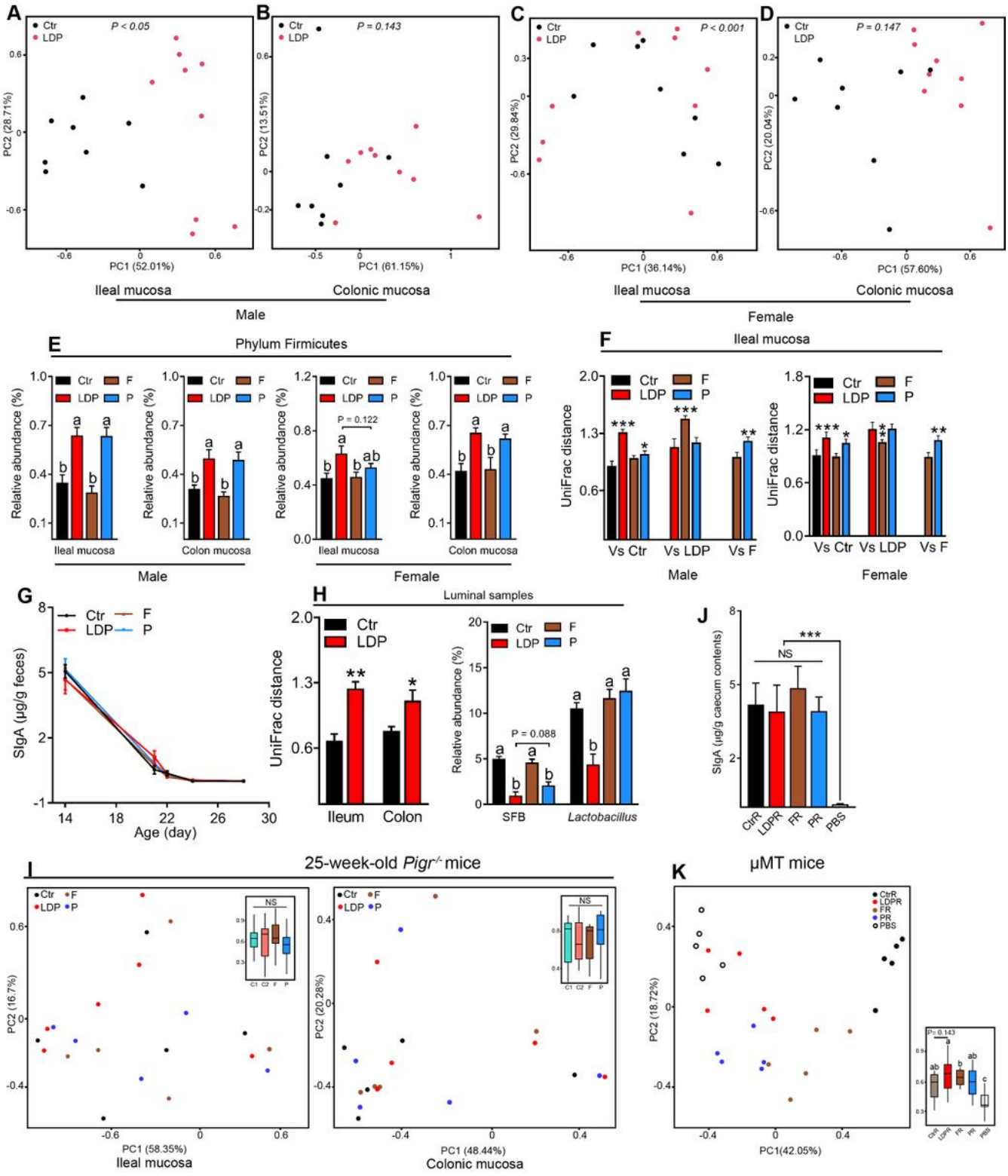

Figure 3

The long-term effects of LDP on intestinal microbiota (A–D) PCoA based on the weighted UniFrac distance showed the differences in the mucosal bacterial compositions of the ileum and colon of 25-week-old LDP and Ctr mice. (E) The relative abundance of the phylum Firmicutes in the mucosal samples of 25-week-old mice. (F) A comparison of the weighted UniFrac distance showed the differences in mucosal bacterial composition in the ileum of 25-week-old mice in all treatments. (G) Changes in fecal

SIgA levels of the Pigr-/- mice, n = 5. (H) Weighted UniFrac distances between the Ctr and LDP mice (left) and the relative abundance of Candidatus Arthromitus and Lactobacillus (right) in 30-d-old Pigr-/- mice, n = 5. (I) PCoA based on the weighted UniFrac distance showed the differences in the mucosal bacterial compositions in 25-week-old Pigr-/- mice after all treatments. (J and K) Changes in the intestinal IgA and ileal microbiota in the μMT mice 12 weeks after the transfer of B cells or PBS, n = 5. (J) Caecal SIgA levels in the μMT mice. (K) The PCoA plot based on weighted UniFrac distance showed the differences in the bacterial composition of the ileal mucosa samples. For A to D, I, and K, the significance was determined using the Wilcox test. For the remaining figures, differences were determined using Mann-Whitney U tests or LSD posthoc tests of one-way ANOVA as compared to Dunnett's test (T3). Different letters indicate a significant difference between columns or points, $p < 0.05$; *$P < 0.05$, **$P < 0.01$, and ***$P < 0.001$.

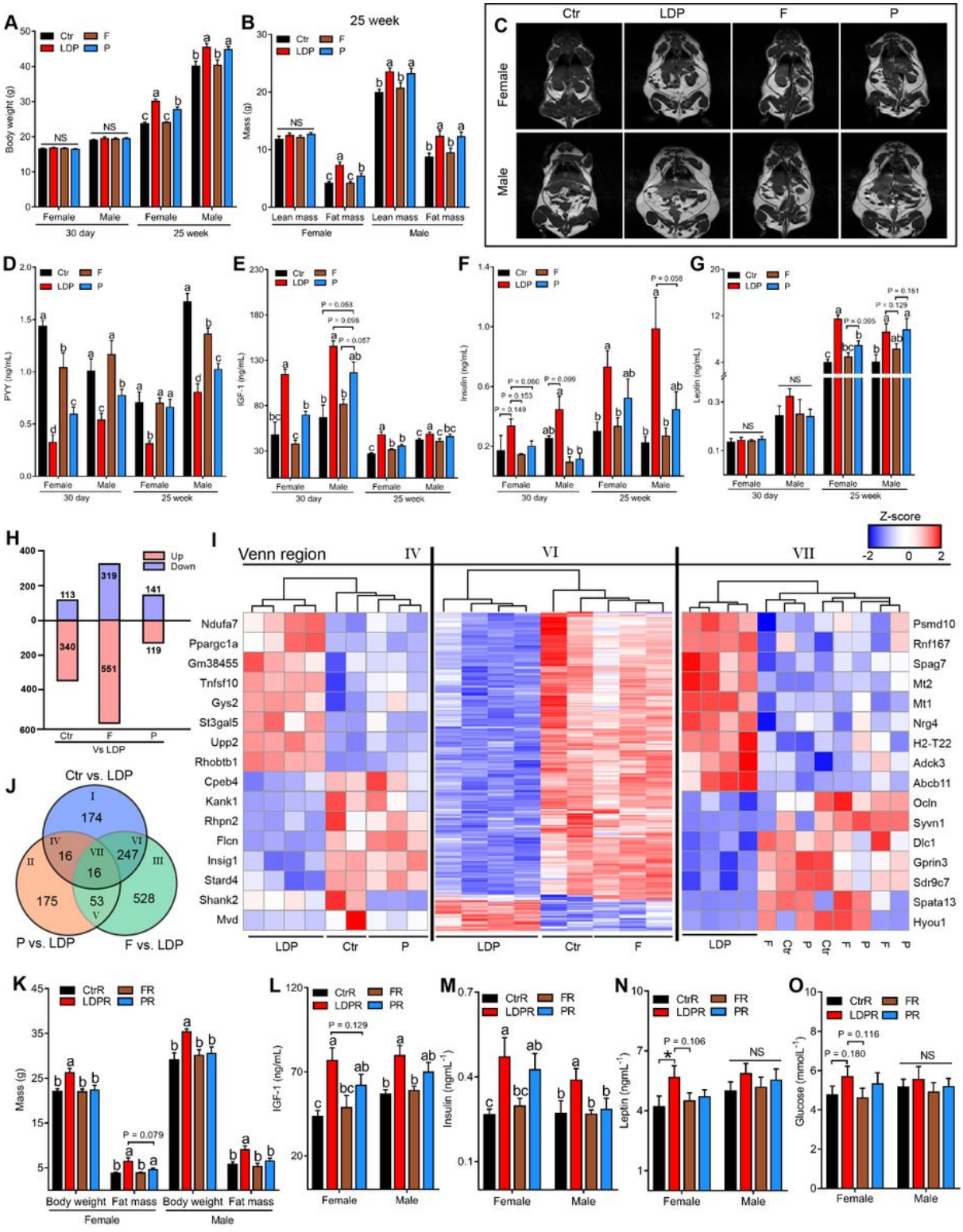

Figure 4

Changes in metabolism. (A–J) Changes in the metabolism of WT SPF mice, where n = 2–4 for the 30-d-old males and females, and n = 8–9 for the 25-week-old males and females. (A) Bodyweight. (B) Lean and fat mass of the 25-week-old mice. (C) Representative MRI images of the 25-week-old mice; the white areas represent lipids, n = 3 for each group. (D–G) Serum hormone concentrations of PYY (D), IGF-1 (E), insulin (F), and leptin (G). (H–J) Transcriptome analysis of the liver in the 30-d-old females, n = 2–4. (H)

The number of genes that exhibit significant (padj < 0.05, |log2 Fold change| > 1.2) hepatic expression differences that were up- or downregulated in the Ctr, F, and P mice compared to the LDP mice. (I) A comparative analysis of differential hepatic gene expression. A Venn diagram indicates the number of overlapping genes in three separate pairwise comparisons. (J) Heatmaps characterize the gene expression values of Venn regions IV, VI, and VII. (K–O) Changes in the metabolism of the 10-week-old WT conventionalized GF mice, where n = 4 for all treatments. (K) Bodyweight and fat mass. (L–N) Serum hormone concentrations of IGF-1 (L), insulin (M), and leptin (N). (O) Fasting serum glucose levels. For all figures except C and H to J, different letters indicate a significant difference between columns, p < 0.05, NS denotes no significant difference; LSD post hoc test or one-way ANOVA as compared to Dunnett's test (T3).

Supplementary Files

This is a list of supplementary files associated with this preprint. Click to download.

- Additionalfile2.docx
- Additionalfile1.docx